Incomplete radiofrequency ablation accelerates proliferation and angiogenesis of residual lung carcinomas via HSP70/HIF-1α

JUN WAN[1], WEI WU[2], YUNLONG HUANG[1], WEI GE[1] and SHANDONG LIU[1]

Departments of [1]Thoracic Surgery and [2]Hematology, The First Affiliated Hospital of Anhui Medical University, Hefei, Anhui 230022, P.R. China

Received January 25, 2016; Accepted March 8, 2016

DOI: 10.3892/or.2016.4858

Abstract. Radiofrequency ablation (RFA) therapy has been proved effective and feasible for lung cancer. However, the molecular mechanisms of local lung cancer recurrence following RFA are poorly understood. The present study aimed to evaluate the ability of HSP70/HIF-1α to affect the proliferation and angiogenesis of non-small cell lung cancers (NSCLCs) following insufficient RFA to uncover the molecular mechanisms of local recurrence. *In vitro* heat treatment was used to establish sublines of NCI-H1650 cells. The NCI-H1650 subline that was established by heat treatment at 54˚C had a relatively higher viability and significantly elevated heat tolerance (compared to the parental strain). After treatment with the HSP70 inhibitor VER-155008, the HIF-1α inhibitor YC-1 and PI3K/Akt inhibitor wortmannin, the viability and proliferation rate of the cells was measured. At the same time, HSP70, HIF-1α and Akt were detected by real-time PCR and western blotting. *In vivo* xenograft tumors were created by subcutaneously inoculating nude mice with NCI-H1650 cells. HSP70, HIF-1α and Akt were detected by western blotting, and CD34 expression was detected by immunohistochemistry before and after RFA or treatment with the VER-155008, YC-1 or wortmannin inhibitors. The heat-adapted NCI-H1650 subline established *in vitro* had a higher viability and proliferative activity compared to parental cells. Inhibiting HSP70/HIF-1α abolished this difference. Blocking the PI3K/Akt signaling pathway decreased HSP70/HIF-1α expression levels. *In vivo*, we found that incomplete RFA treatment promoted HSP70/HIF-1α and CD34 expression. Additionally, the combination of RFA and treatment targeting HSP70/HIF-1α resulted in a synergistic reduction in tumor growth compared to incomplete RFA alone. The PI3K/Akt signaling pathway is also involved in regulating HSP70/HIF-1α expression during this process. We conclude that the accelerated proliferation and angiogenesis potential of residual lung carcinomas following RFA treatment was induced by HSP70/HIF-1α, expression of which is regulated by the PI3K/Akt signaling pathway.

Correspondence to: Dr Jun Wan, Department of Thoracic Surgery, The First Affiliated Hospital of Anhui Medical University, 218 Jixi Road, Hefei, Anhui 230022, P.R. China
E-mail: junwandr@yahoo.com

Abbreviations: RFA, radiofrequency ablation; NSCLC, non-small cell lung cancer; HIF-1α, hypoxia inducible factor-1α; HSP70, heat shock protein 70; MVD, microvessel density

Key words: radiofrequency ablation, non-small cell lung cancers, hypoxia inducible factor-1α, heat shock protein 70

Introduction

Lung cancer is the most common and fatal cancer worldwide (1). In China, lung cancer has been the leading cause of cancer-related deaths since the 1990s (2). Recent trend analyses indicate that the incidence of lung cancer has increased over the last 20 years, and it is predicted that the disease burden may continue to increase if no effective action is taken to control lung cancer (3). In addition, the lungs are the second most frequent site of metastasis, and metastases to the lung complicate the course of as many as 40% of other malignancies (4). For the treatment of lung cancer, surgical resection, consisting of a lobectomy and complete lymph node dissection, has long been considered the standard treatment for resectable tumors and offers the best curative chance for long-term survival (5). However, it is estimated that only a third of patients with non-small cell lung cancer (NSCLC) are suitable for curative resection (6). Therefore, non-invasive local treatments that makes it possible to avoid resection of the functioning parenchyma or prolonged general anaesthesia represent a key point in the management of patients who are not eligible for surgery (7).

As a minimally invasive approach for the local treatment of lung cancer, radiofrequency thermal ablation (RFA) has recently received much attention. RFA is a new image-guided percutaneous technique that utilizes hyperthermic energy (8). Studies indicate that lung tumors are ideal targets for RFA since the surrounding air in the adjacent normal lung parenchyma provides an insulating effect, concentrating the RF energy within the tumor tissue (9). The major problem with RFA treatment is that thermal destruction may occur before achieving complete tumor destruction (10). According to a previous study, lung RFA is associated with increased rates of local recurrence in tumors with large volumes since it is

difficult to reach sufficiently high temperatures further away from the heat source, particularly in the treatment of larger tumors (11). Moreover, the rich blood supply of the tumor is another cause for local recurrence, since an abundant blood supply may help to dissipate the thermal energy and weaken the ablation effect (12). A greater number of clinical cases concerned with the over-growth of residual tumors after RF ablation have been reported (11,13). Ke *et al* confirmed that low RFA temperatures at target sites could facilitate the rapid progression of residual hepatic VX2 carcinomas (14). Cumulative evidence has demonstrated that residual tumors present after RFA may exhibit an aggressive phenotype with an unfavorable prognosis, eventually leading to the deterioration of the patient overall condition.

However, the specific molecular mechanisms by which overproliferation of residual lung tumor cells occurs following RFA are still unclear. Hypoxia-inducible factor-1α (HIF-1α), a key transcriptional regulator, plays a central role in the adaptation of tumor cells to hypoxia by activating the transcription of genes that regulate several biological processes including angiogenesis, cell proliferation and migration (15). In our pervious study, we found that HIF-1α can regulate the expression of multiple cytokines, such as vascular endothelial growth factor-A (VEGF-A) (16), while promoting the proliferation and angiogenesis potential of small cell lung cancers (SCLCs) (17). Heat-shock proteins (HSPs) are known to serve as protein chaperones that assist in protein folding, assembly, degradation and translocation. HSP70 is a member of the HSP family, and it is constitutively expressed at low levels in most tissues (18). The expression of HSP70 is also significantly upregulated under thermal stimulation (19). Previous studies indicate that HSP70 interferes with the signaling pathways and cellular responses to hypoxic stress; HIF-1α stability is influenced by HSP70, which forms a long-lasting complex with HIF-1α to increase the lifespan of HIF-1α (20). As far as the regulatory mechanism, Yeh *et al* showed that PI3K/Akt contributes to promoting HIF-1α expression by upregulating the expression of HSP70 (21). In the present study, we hypothesized that insufficient RFA promoted the proliferation and angiogenesis potential of residual lung cancer cells, which plays an important role in the rapid proliferation of residual tumor cells after RFA. Then, we investigated whether local hyperthermia could change the microenvironment of ablated tumor tissues and the biological characteristics of residual tumor cells. We found that these cells exhibited rapid proliferation and upregulated angiogenesis potential through a HSP70/HIF-1α-dependent mechanism.

Materials and methods

Materials. The PI3K/Akt inhibitor wortmannin (22), the HSP70 inhibitor VER-155008 (23) 5'-O-(4-cyanobenzyl)-8-[(3,4-dichlorobenzyl)amino]adenosine, the HIF-1α inhibitor YC-1 (24) and 3-[4,5-dimethylthiazol-2-yl]-2,5-diphenyltetrazolium bromide (MTT) were purchased from Sigma-Aldrich (St. Louis, MO, USA). TRIzol reagent was purchased from Invitrogen Corp. (Carlsbad, CA, USA). RIPA lysis buffer was purchased from Beyotime Institute of Biotechnology, China. Anti-HIF-1α used at a 1:500 dilution, anti-HSP70 used at a 1:1,000 dilution, and anti-Akt used at a 1:1,000 dilution were purchased from Cell Signaling Technology (Beverly, MA, USA). Anti-CD34 used at a 1:50 dilution was purchased from Wuhan Boster Biological Engineering Technology Ltd., Co. (Wuhan, China).

Cell lines and cell culture. According to our previous study (16,17), the human NSCLC NCI-H1650 cell line was maintained in RPMI-1640 medium (Sigma-Aldrich) supplemented with 10% fetal bovine serum (FBS), 100 U/ml penicillin and 100 μg/ml kanamycin at 37˚C in a humidified atmosphere containing 5% CO_2 and 20% O_2. The medium was routinely changed 2-3 days after seeding. Cells were detached with trypsin/EDTA (Gibco-BRL, Paisley, UK) and resuspended in a 1:1 solution of serum-free RPMI-1640 medium to a final concentration of ~$5x10^5$ cells/10 μl.

Heat treatment of lung cancer cells and establishment of the sublines. In all of the experiments, the cells were exposed to hyperthermic stress during the exponential phase in cell culture plates. The NCI-H1650 cells were seeded into cell culture plates. After 24, 48 or 72 h of incubation they were exposed to heat stress. The plates were sealed with parafilm and submerged in a water bath at the desired temperature for 10 min. Eight temperatures ranging from 42-70˚C were selected: 42, 46, 50, 54, 58, 62, 66 and 70˚C. These temperatures match the ablation temperatures applied during the clinical treatment of lung cancer. After the hyperthermic treatment, fresh culture medium was added to each well, and the surviving cells were maintained at 37˚C in an atmosphere containing 5% CO_2 and 20% O_2. These cells separately cultured under 8 desired temperature points were utilized as 8 sublines. One subline was generated from each heat treatment.

MTT assay for lung cancer cell viability. According to the study of Kong *et al* (25), cells were cultured at a concentration of $1x10^4$ cells/well in 48-well plates. MTT solution was added to each well at a final concentration of 0.5 mg/ml and incubated for 4 h. At the end of the incubation, formazan crystals resulting from MTT reduction were dissolved by addition of 150 ml dimethyl sulfoxide (DMSO)/well. The optical density (OD) was read at 570 nm, and the average values were determined from replicate wells.

Real-time PCR analysis of HSP70 and HIF-1α. Real-time PCR was performed using a SYBR ExScript RT-PCR kit according to the manufacturer's protocol (Takara Biotechnology Co., Ltd., Dalian, China) and the iCycler Real-Time PCR Detection System (Bio-Rad Laboratories, Hercules, CA, USA). All the RNA samples were extracted and run in duplicate on 96-well optical PCR plates. The thermal cycling conditions were as follows: 1 cycle of 90.0˚C for 10 min, 40 cycles of 95.0˚C for 5 sec, 60.0˚C for 30 sec and 81 cycles of 55.0˚C for 10 min (with an increase set point temperature after cycle 2 of 0.5˚C). β-actin was used as an internal control. PCR primer sequences were as follows: HSP70 sense, 5'-CTG ACAAGAAGAAGGTGCTGG-3' and antisense, 5'-AGCAGC CATCAAGAGTCTGTC-3', HIF-1α sense, 5'-CATCAGCTAT TTGCGTGTGAGGA-3' and antisense, 5'-AGCAATTCATCT GTGCTTTCATGTC-3'.

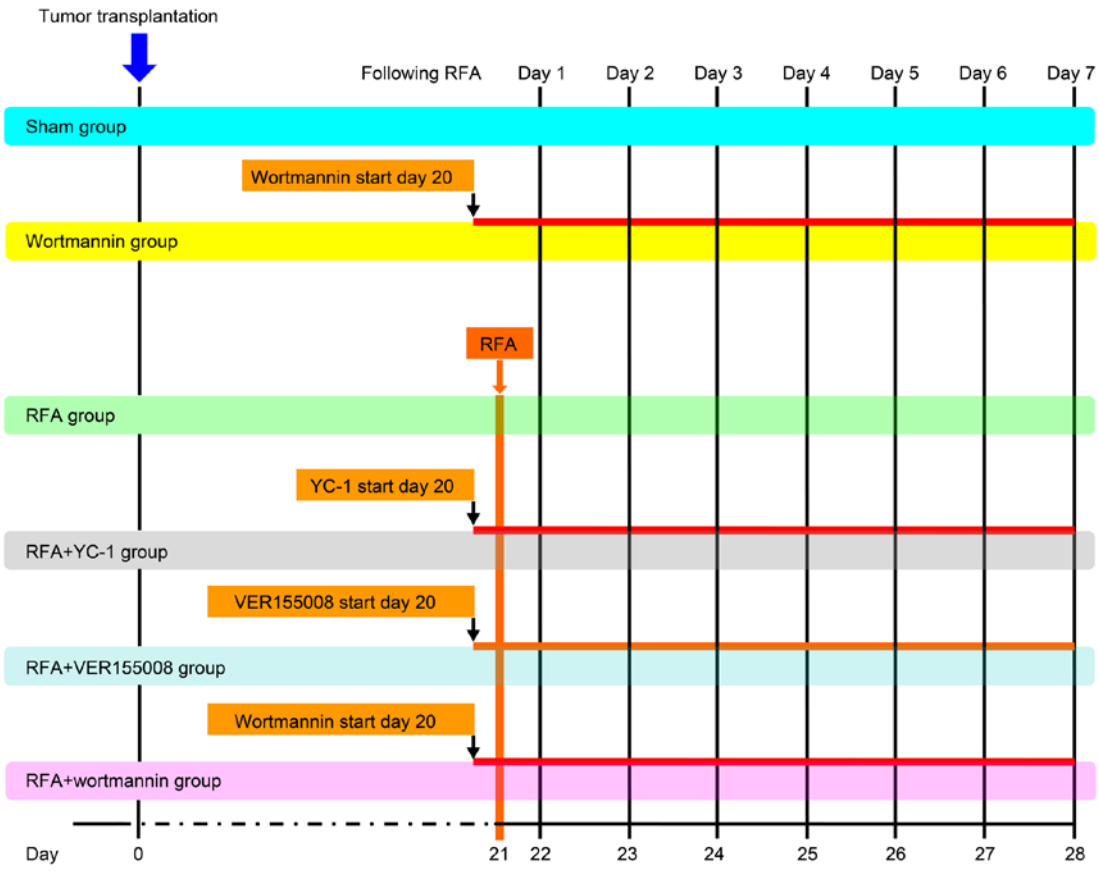

Figure 1. Treatment groups and schedule.

Western blot analysis. Cells were harvested and analyzed for the expression of HIF-1α, HSP70, Akt and p-Akt. Briefly, proteins were extracted by disrupting cells in RIPA lysis buffer, were separated on polyacrylamide gels, and transferred to polyvinylidene difluoride (PVDF) membranes. The membranes were then blocked at room temperature for 1 h with 5% non-fat milk in Tris-buffered saline containing Tween-20 (TBST). Then, the membranes were incubated with anti-HIF-1α, anti-HSP70, anti-Akt, anti-phospho-Akt primary antibodies at 37˚C for 2 h. After, the membranes were incubated with peroxidase-conjugated IgG at room temperature for 1 h. The membranes were subsequently incubated with goat anti-rabbit peroxidase-conjugated secondary antibodies, and immunoreactivity was detected using an enhanced chemiluminescence kit and captured on X-ray film. β-actin was used as an internal normalization control.

Establishing xenografts in nude mice and RFA treatment. Male congenital athymic BALB/c nude mice were obtained from the Experimental Animal Center of the Shanghai Jiao Tong University School of Medicine and maintained under pathogen-free conditions in accordance with established institutional guidance and approved protocols. All experiments were carried out using 6- to 8-week-old mice weighing 16-22 g. *In vitro* cultured NCI-H1650 cells ($1x10^7$) at a final concentration of ~$5x10^5$ cells/10 μl were suspended in phosphate-buffered saline (PBS) and were subcutaneously injected into the flank area of mice. After tumors reached 3-5 mm in diameter, mice were injected with 10% DMSO/PBS, 4 mg/kg twice weekly.

For RFA treatment, we applied the method of Xu *et al* (26). RFA was performed using a bipolar RFA device (Blade Opto-Electronic Technology Development Co., Ltd., Beijing, China), which is a microRFA probe with an active tip length of 10 mm. To simulate the clinical settings of tumor recurrence following RFA, the 'incomplete RFA' strategy using 180 sec of RFA at 1 W power was applied when the size of the tumor reached nearly 3.3-3.6 cm^3 on the 21st day of tumor growth. This procedure resulted in incomplete ablation of the tumors.

There were a total of 80 mice involved in the experiment, which were divided into 6 groups: control (sham puncture using an identical probe without applying energy), RFA, VER-155008 + RFA (50 μg/day injection), YC-1 + RFA (600 μg/day injection), wortmannin (0.07 mg/day injection) and wortmannin + RFA groups (0.07 mg/day injection). Each group contained 10 mice (evenly divided into female and male genders). We measured the tumor size daily with calipers from days 1-7 following RFA treatment, and tumor volume was calculated according to the formula: Volume = $width^2$ x length x 0.5. All treatment groups and schedules are shown in Fig. 1.

Immunohistochemistry detection for CD34. Tissue sections of 4 μm were prepared and endogenous peroxidases were inhibited with 0.3% hydrogen peroxide in methanol for 30 min. Antigen retrieval was achieved using 0.05% protease XIV

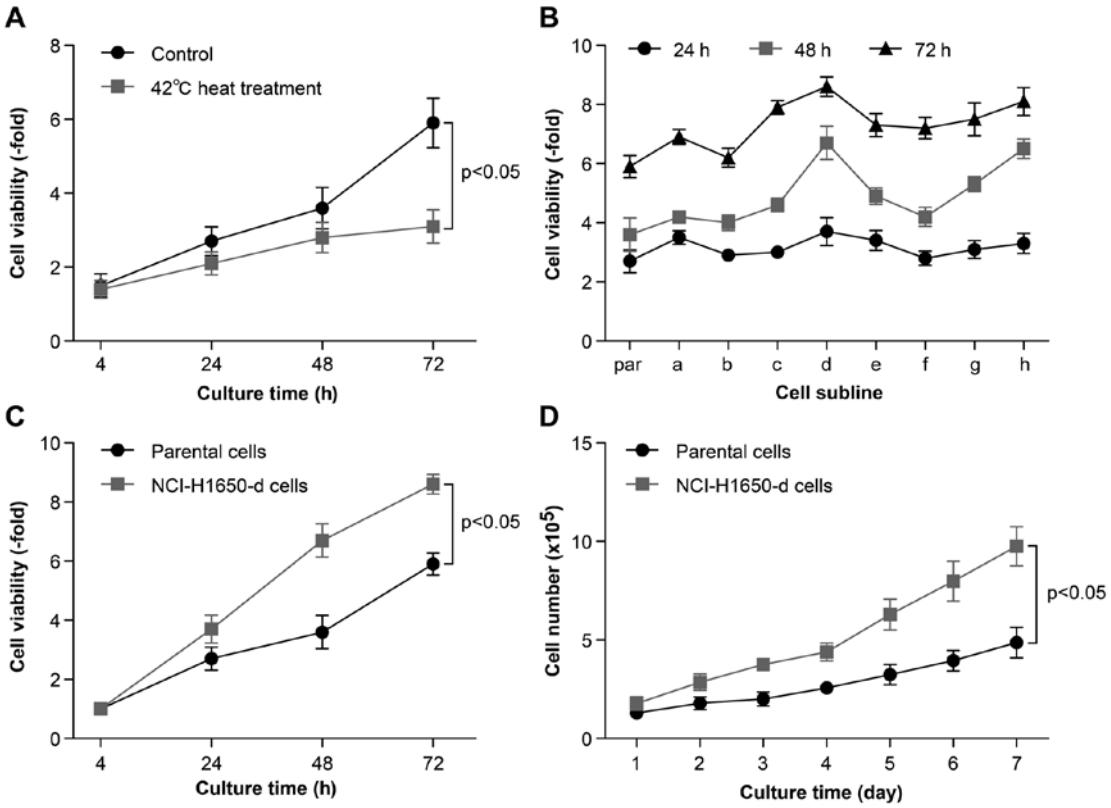

Figure 2. The viability of NCI-H1650 cells and sublines derived from NCI-H1650 cells after hyperthermia. (A) NCI-H1650 cells were cultured after 42˚C heat treatment. The 24, 48 and 72 h cell viability of NCI-H1650 cells with or without 42˚C heat treatment were measured using MTT assay ($p<0.05$, control group vs. 42˚C heat treatment group). (B) Eight sublines were established following 42, 46, 50, 54, 58, 62, 66 and 70˚C heat treatment for 15 min as described in Materials and methods. The 24, 48 and 72 h viability was evaluated by MTT assay after these 8 sublines had been established. par, parental NCI-H1650 cells; a-h, sublines derived from the NCI-H1650 cells. (C) The 24, 48 and 72 h viability of parental NCI-H1650 and 54˚C heat-adapted NCI-H1650 cells was evaluated by MTT assay ($p<0.05$, parental NCI-H1650 cells vs. NCI-H1650-d cells). (D) A growth curve of parental NCI-H1650 and NCI-H1650-d cells was drawn. Data are the representative results of three independent experiments ($p<0.05$ from day 2-7 parental NCI-H1650 cells vs. NCI-H1650-d cells).

at 37˚C for 5 min. Sections were incubated with the mouse anti-human CD34 primary antibody overnight at 4˚C, then the slides were incubated with rabbit anti-mouse secondary antibody at room temperature for 45 min. The sections were subsequently incubated with a streptavidin-biotin-peroxidase complex (Vectastain ABC kit; Vector Laboratories, Burlingame, CA, USA) at room temperature for 45 min. The reaction was visualized using chromogen diaminobenzidine (DAB) for 10 sec. Finally, the slides were counterstained with hematoxylin, and then mounted and examined on a Nikon Eclipse Ti microscope with a 40x objective. Microvessel density (MVD) was defined as the number of positively stained vessels per high-power field of view (HPF).

Statistical analysis. SPSS 13.0 software (SPSS, Inc., Chicago, IL, USA) was applied to complete data processing. Independent-sample t-tests were used to evaluate the differences in OD values. All data are represented as mean ± SD for three independent experiments. Results were considered statistically significant when the p-value was <0.05.

Results

In vitro heat treatment generates NCI-H1650 cell sublines with increased viabilities and proliferation activities. To detect the potential effect of hyperthermia on the proliferative activity of lung cancer cells, first we monitored cell viability at 24, 48 and 72 h after incubation at 42˚C for 10 min. We found that the viability of the NCI-H1650 cells after incubation at 42˚C was significantly decreased compared to cells that did not receive heat treatment; this may be due to cell apoptosis and death. However, the cellular viability of the parental cells not undergoing hyperthermia treatment and the cells cultured at 42˚C reached their highest viability at 72 h of incubation (Fig. 2A). In addition, the cell viability of NCI-H1650 cells after various heat treatments was assessed in continuously passaged cells following exposed to 8 different heat conditions denoted in the methods. The cellular viability of these 8 sublines was tested at 24, 48 and 72 h of incubation. We found that these sublines exhibited significant differences in cell viability compared to their parental cells, particularly NCI-H1650 cells adapted to 54˚C, which were significantly more viable than their parental cells (Fig. 2B and C). We continued to monitor the differences in proliferation activity between parental lung cancer cells and these NCI-H1650 cell sublines. After this subline was established, we cultured the cells for 7 days, drawing a proliferation curve. From the proliferation curve, we found that NCI-H1650 cells adapted to 54˚C exhibited a significantly higher proliferation rate compared to the parental cells (Fig. 2D). Therefore, we conclude that thermal treatment can partially kill NCI-H1650 cells, while generating sublines with increased viability and proliferation

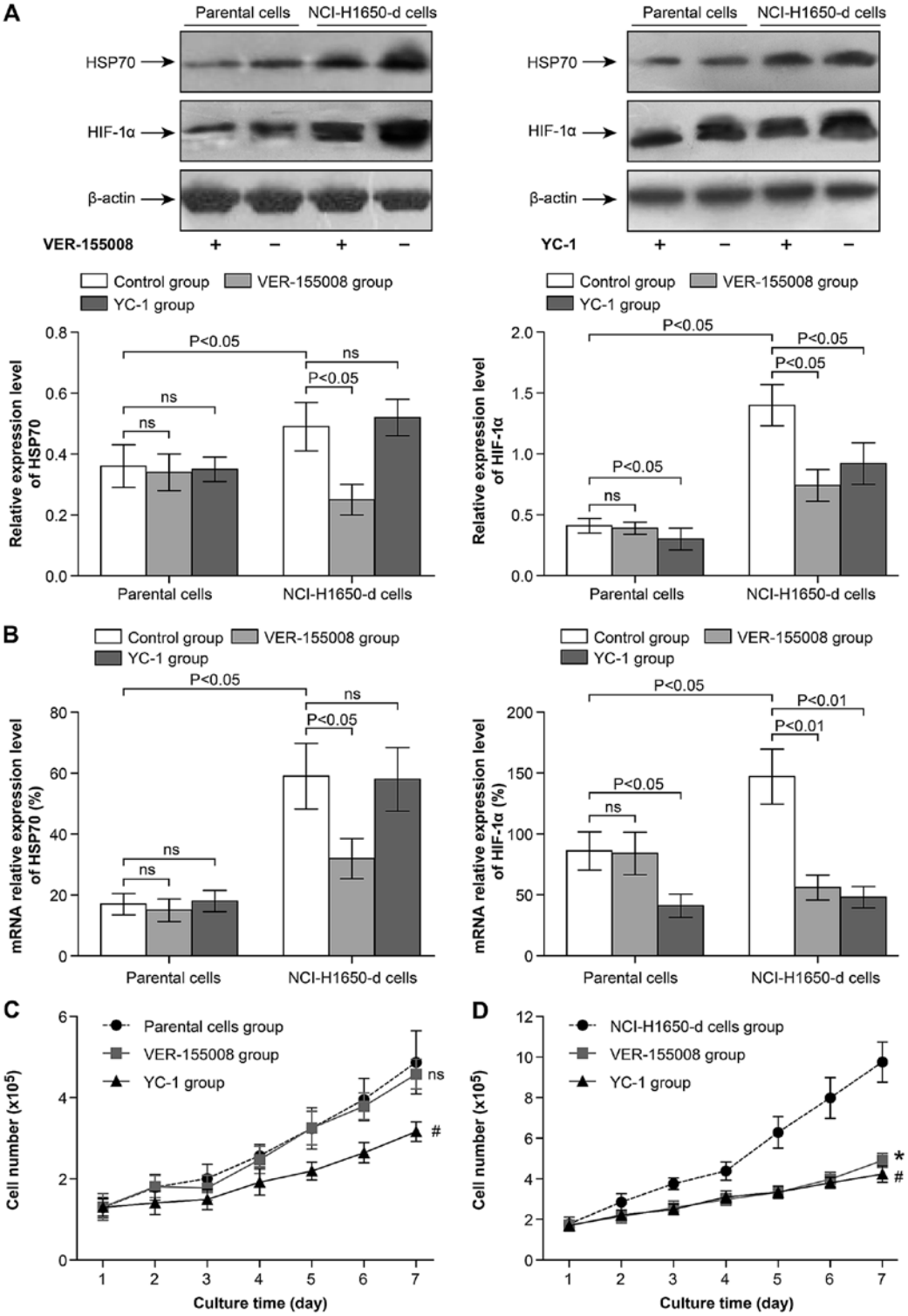

Figure 3. (A) Heat-adapted NCI-H1650 cells (54˚C) express elevated levels of HSP70 and HIF-1α. (A) Expression of HSP70 and HIF-1α in parental NCI-H1650 and NCI-H1650-d cells treated with or without VER-155008 (50 μg) or YC-1 (20 μg) for 24 h was analyzed by western blot and semi-quantitative analyses. (B) The mRNA expression of HSP70 and HIF-1α in parental NCI-H1650 and NCI-H1650-d cells treated with or without VER-155008 (50 μg) or YC-1 (20 μg) was assayed using real-time PCR. (C) Growth curve of parental NCI-H1650 cells treated with or without VER-155008 or YC-1 (ns, parental cell group vs. VER-155008 group day 2-7; $^{\#}$p<0.05, parental cell group vs. YC-1 group day 2-7. (D) Growth curve of NCI-H1650-d cells treated with or without VER-155008 or YC-1 (*p<0.05, NCI-H1650-d cells vs. VER-155008 day 2-7; $^{\#}$p<0.05, NCI-H1650-d cell group vs. YC-1 group day 2-7). ns, no significance.

activity. Therefore, we used the NCI-H1650 subline adapted to 54˚C for our subsequent research.

HSP70/HIF-1α are involved in regulating the viability and proliferation activity of NCI-H1650 sublines. We further investigated the differences between heat-adapted strains and parental lung cancer cells. Western blotting demonstrated that the protein levels of HSP70 and HIF-1α were upregulated in the NCI-H1650 cells adapted to 54˚C compared to the parental cells (Fig. 3A). At the same time, the mRNA levels of HSP70

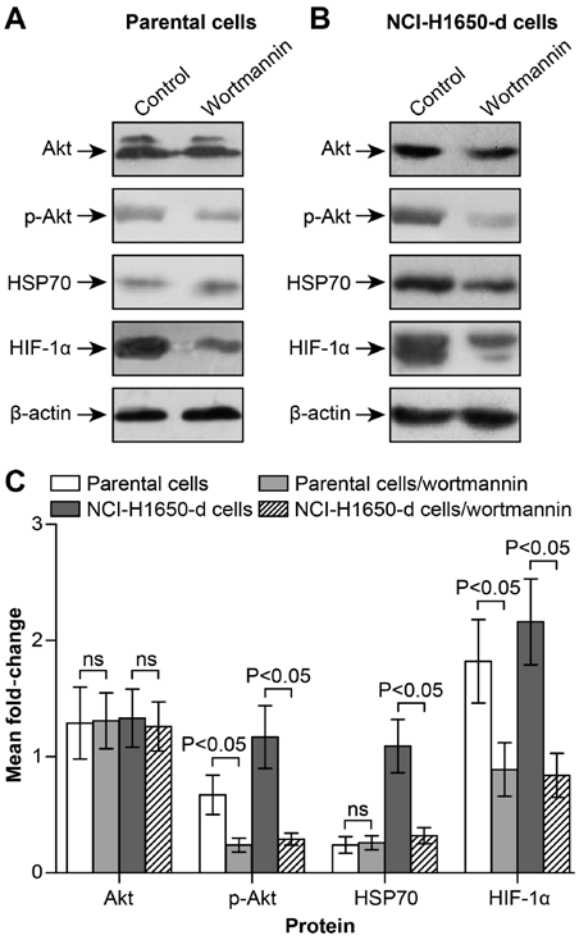

Figure 4. The PI3K/Akt signaling pathway is involved in regulating HSP70 and HIF-1α expression. (A) The expression levels of Akt, p-Akt, HSP70 and HIF-1α in parental NCI-H1650 cells treated with or without wortmannin (20 μM) for 24 h were analyzed by western blotting. (B) The expression levels of Akt, p-Akt, HSP70 and HIF-1α in heat-adapted cells treated with or without wortmannin (20 μM) for 24 h were analyzed by western blotting. (C) Semi-quantitative analysis of Akt, p-Akt, HSP70 and HIF-1α expression. ns, no significance.

and HIF-1α were also increased in the heat-adapted cells compared to the parental cells (Fig. 3B). The HSP70 inhibitor VER-155008 significantly decreased the protein and mRNA expression of HSP70 and HIF-1α in the heat-adapted cells, but did not inhibit the expression in the parental cells (Fig. 3A and B). Subsequently, we found that treatment with VER-155008 or YC-1 significantly inhibited the proliferation activity of the NCI-H1650 heat-adapted cells (Fig. 3D). However YC-1, but not VER-155008, inhibited the proliferation activity of the parental NCI-H1650 cells (Fig. 3C). These data indicate that the proliferation activity of the heat-adapted NCI-H1650 cells was regulated by HSP70/ HIF-1α, but the proliferation activity of the parental cells was not linked to HSP70.

HSP70/HIF-1α expression is regulated by the PI3K/Akt signaling pathway in heat-adapted NCI-H1650 cells. Western blot detection and semi-quantitative analyses demonstrated that applying specific inhibitors of PI3K/Akt (wortmannin) inhibited the expression of Akt phosphorylated active form-p-Akt, but had little effect on the total expression of Akt protein (Fig. 4A-C). Wortmannin intervention also revealed the inhibition of HSP70 or HIF-1α expression in the heat-adapted cells (Fig. 4B and C). However, for the parental NCI-H1650 cell line, inhibiting PI3K/Akt signaling pathway significantly inhibited HIF-1α protein expression (Fig. 4A and C). However, inhibiting PI3K/Akt did not inhibit HSP70 expression at the protein level in the parental cells (Fig. 4B). We conclude that PI3K/Akt contributes to the reduction in HIF-1α expression by inhibiting expression of HSP70 in heat-adapted cell lines. However, for the parental lung cancer cells, PI3K/Akt signaling directly regulated HIF-1α expression, and this biological process was not associated with HSP70.

HSP70/HIF-1α are involved in the proliferation and angiogenesis of residual lung carcinomas following incomplete RFA. At day 20 post-tumor implantation, no differences in tumor size were observed, and the size of tumors in each group was 3.3-3.6 cm^3. Tumors were then subjected to RFA treatment (Fig. 5A). From days 1-7 following RFA treatment, the tumor size was daily measured. According to the slope of the growth curve, animals subjected to RFA treatment showed a significantly increased growth rate compared to the control group. These results indicate that RFA treatment may induce residual tumor growth (Fig. 5B). From day 1-7 following RFA treatment, there was a significant size reduction in tumors in the VER-155008 + RFA and YC-1 + RFA groups compared with the RFA only group (Fig. 5B). These data indicate that HSP70/HIF-1α is involved in residual tumor growth.

At day 7 following RFA treatment, tumors were resected for western blot analysis. We found that HSP70 and HIF-1α were significantly upregulated in the RFA group when compared to the control group (Fig. 5C). After VER-155008 intervention, HSP70 and HIF-1α were both inhibited; expression in the VER-155008 + RFA group was significantly decreased when compared with the RFA group (Fig. 5C). However, after YC-1 intervention, HIF-1α expression was inhibited, but HSP70 expression did not significantly change (Fig. 5C). Thus, we conclude that the HIF-1α expression may be regulated by HSP70 in lung carcinomas following incomplete RFA. However, in the VER-155008 group, without RFA treatment, HSP70 and HIF-1α expression showed little change compared with the control group. However, in the YC-1 group, HIF-1α expression was inhibited but HSP70 expression did not significantly change compared with the control group (Fig. 5C).

At day 7 following RFA treatment, the tumors were resected and MVD (CD34-positive expression) was detected by immunohistochemistry staining to analyze angiogenesis potential (Fig. 5D). We found that RFA treatment significantly stimulated the angiogenesis potential of tumors compared to tumors not treated with RFA (Fig. 5D). However, with VER-155008 or YC-1 intervention to inhibit HSP70 and HIF-1α, respectively, the angiogenesis potential of the tumor was also significantly inhibited; MVD was attenuated in the VER-155008 + RFA and the YC-1 + RFA groups compared with the RFA group. However, in the VER-155008 group, MVD expression did not significantly change, while it was significantly inhibited in the YC-1 group compared to the control group (Fig. 5D). Therefore, HIF-1α expression appeared to be regulated by HSP70, while its expression inhibited the angiogenesis and proliferation of residual lung carcinomas following incomplete RFA. However, in tumors

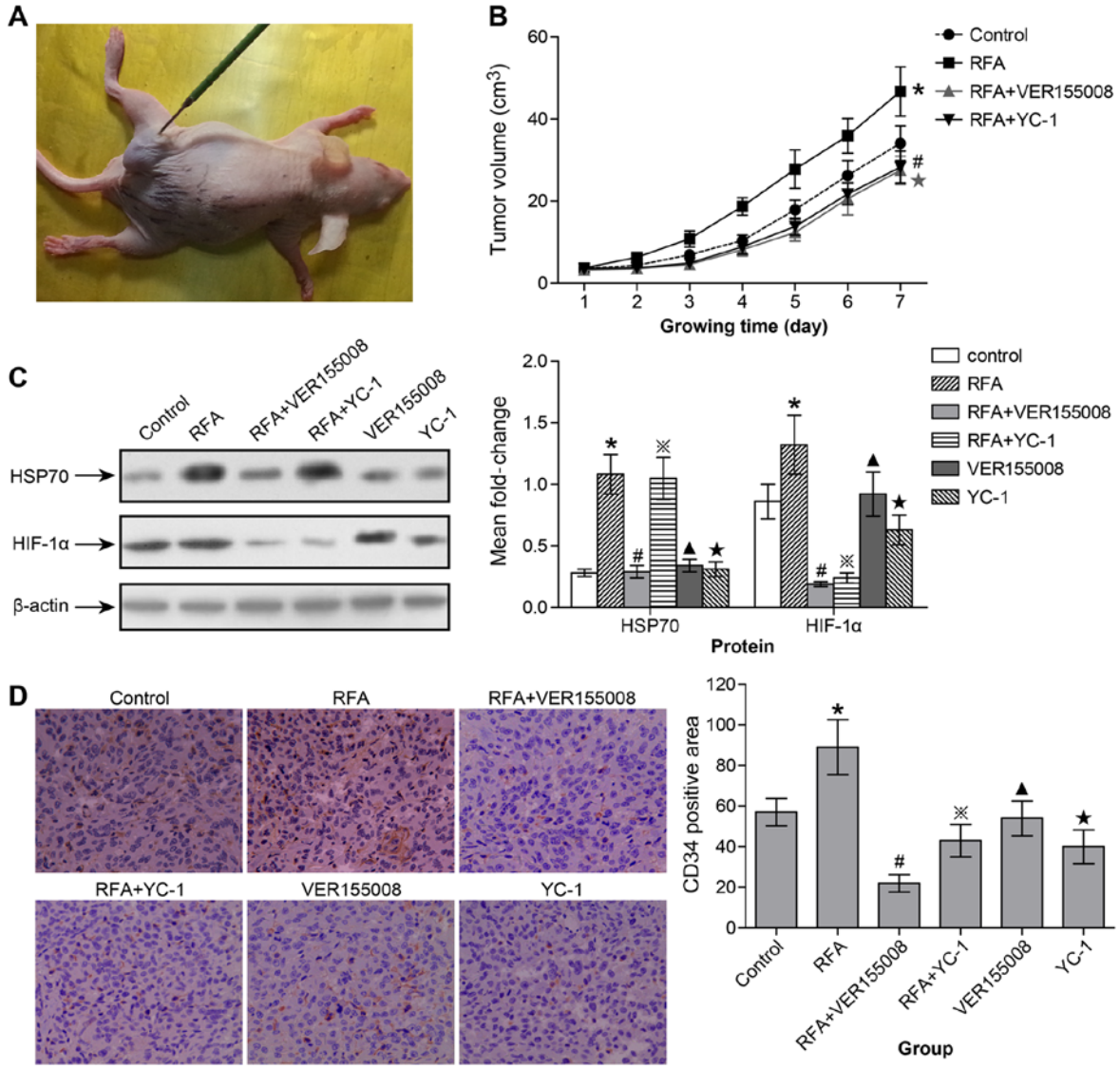

Figure 5. HSP70/HIF-1α are involved in proliferation and angiogenesis of subcutaneously transplanted tumors following incomplete radiofrequency ablation. (A) After the subcutaneously transplanted tumor had formed, the RFA probe was inserted into the tumor tissue. (B) Growth curve of subcutaneously transplanted tumors in control, RFA, VER-155008 + RFA and YC-1 + RFA group (*p<0.05 from day 3-7 control group vs. RFA group; ⋆p<0.05 from day 3-7 RFA group vs. VER-155008 + RFA group; #p<0.05 from day 3-7 RFA group vs. YC-1 + RFA group). (C) In the control, RFA, VER-155008 + RFA, YC-1 + RFA, VER-155008 alone and YC-1 alone groups, HSP70 and HIF-1α expression in subcutaneously transplanted tumors was measured by western blot and semi-quantitative analyses (*control group vs. RFA group: HSP70, p<0.05; HIF-1α, p<0.05. #RFA group vs. VER-155008 + RFA group: HSP70, p<0.05; HIF-1α, p<0.01. ※RFA group vs. YC-1 + RFA group: HSP70, ns; HIF-1α, p<0.01. ▲Control group vs. VER-155008 group: HSP70, ns; HIF-1α, ns. ★Control group vs. YC-1 group: HSP70, ns; HIF-1α, p<0.05). (D) At day 7 following RFA treatment, the numbers of new microvessels marked with CD34 expression in the subcutaneous tumors were detected by immunohistochemistry analysis and quantified by performing counts of 10 random fields at a magnification of x400 (*p<0.05 control group vs. RFA group; #p<0.05 RFA group vs. VER-155008 + RFA group; ※p<0.05 RFA group vs. YC-1 + RFA group; ▲ns control group vs. VER-155008 group; ★p<0.05 control group vs. YC-1 group). ns, no significance.

not treated with RFA, HSP70 did not appear to be involved in this regulatory process.

Targeting the PI3K/Akt signaling pathway inhibits tumor growth and HSP70/HIF-1α expression after RFA treatment in nude mice. Considering the potential role of the PI3K/Akt signaling pathway in HSP70/HIF-1α expression, we wanted to better understand the involvement of Akt in the stability regulation of HSP70/HIF-1α. To confirm that HSP70/HIF-1α downregulation occurs by interfering with PI3K/Akt signaling and to exclude potential side-effects of inhibitory drugs, we applied a specific inhibitor of PI3K/Akt signaling, called wortmannin. Following RFA treatment, the tumor size was again measured from day 1-7 and resected at day 7 for western blot analysis. We found that the combination of wortmannin intervention with RFA treatment significantly decreased HSP70 and HIF-1α expression (Fig. 6A). At the same time, a significant reduction in the size of the tumor was observed in the wortmannin + RFA group compared with the RFA group over the course of the 7 days of observation (Fig. 6B). However, in the wortmannin group we found that the HIF-1α expression level and tumor volume were significantly decreased, while HSP70 expression was largely unaffected compared to the control group (Fig. 6A and B). Thus, we suspected that following incomplete RFA treatment, the PI3K/Akt signaling pathway may play a central role in regulating HSP70/HIF-1α

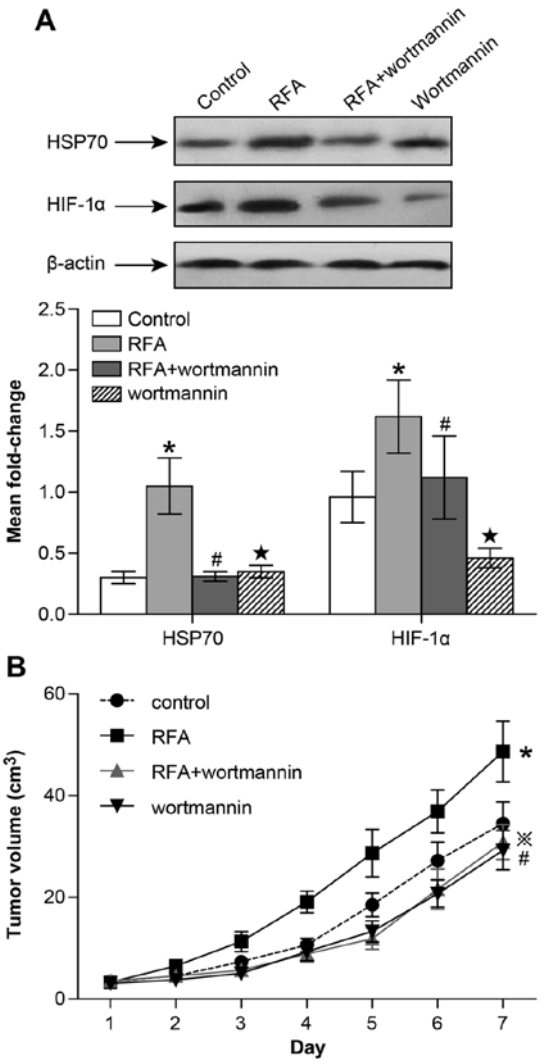

Figure 6. The PI3K/Akt signaling pathway regulates HSP70/HIF-1α expression and residual tumor growth following incomplete radiofrequency ablation. (A) In the control, RFA, wortmannin + RFA and wortmannin groups, HSP70 and HIF-1α expression in the subcutaneously transplanted tumors was measured by western blot and semi-quantitative analyses (*control group vs. RFA group: HSP70, p<0.05; HIF-1α, p<0.05; #RFA group vs. wortmannin + RFA group: HSP70, p<0.05; HIF-1α, p<0.05; ★control group vs. wortmannin group: HSP70, ns; HIF-1α, p<0.05). (B) Growth curve of subcutaneously transplanted tumors in the control, RFA, wortmannin + RFA and wortmannin group (*p<0.05 from day 3-7 control group vs. RFA group; ※p<0.05 from day 3-7 RFA group vs. wortmannin + RFA group; #p<0.05 from day 3-7 control group vs. wortmannin group).

expression, which affects the growth of the residual tumor. However, in tumors not undergoing RFA treatment, PI3K/Akt signaling may directly regulate HIF-1α expression, while heat-induced HSP70 is not involved.

Discussion

Radiofrequency ablation (RFA) is becoming an increasingly accepted treatment for primary lung cancer in patients who are not candidates for subsegmental resection or lobectomy (27). Compared to radiotherapy and chemotherapy, RFA is focused exclusively on the tumor area without causing any damage to the normal surrounding tissue. Compared to surgical treatment, it is superior in that it is minimally invasive. For advanced lung cancers, including SCLCs, RFA can also be maximally effective for palliative care (28). In its early stage, it is not clear whether RFA may function best as a stand-alone therapy or in combination with other modalities. Understanding and recognizing the patterns of tumor recurrence is critical in evaluating the efficacy of this new treatment and to determine optimal candidates for this treatment (29).

Although most studies indicate that lung RFA is safe and feasible, operation complications appear to be common in clinical trails. The most common complication is pneumothorax or hemothorax. However, with the progression of hemostasis techniques and the improvements in surgical repair materials, the incidence of these complications has been significantly reduced (30). Nevertheless, such as other therapeutic methods, postoperative recurrence is still a challenging problem to solve for the RFA treatment of lung cancers. Follow-up imaging data indicate that local treatment area, intrapulmonary and nodal recurrences are commonly found during the first 2 years after RFA, and that the most common area of recurrence would be the local treatment area (27). Increasing tumor sizes and stages have been significantly associated with the likelihood of recurrence with RFA. Giraud *et al* proposed that microscopic extensions of primary lung cancers should be encompassed in a margin of 8 mm for adenocarcinomas and 6 mm for squamous cell carcinomas. The aim of ablation should be to include an expected ablation zone that includes the primary tumor plus at least an additional 8-10 mm beyond the visible tumor margin in all directions. Therefore, the target ablation diameter should be 1.6-2 cm greater than the tumor diameter (31). Various scholars suggest that it is very difficult to achieve complete ablation due to heat sink effects from adjacent vessels or the tumor angiogenesis network (32). However, a new opinion was brought forward that local recurrence following RFA may be the result of the rapid growth of residual tumor cells, which has been observed in numerous clinical centers (23).

Various studies demonstrate that residual tumor cells are prone to proliferation, invasion and metastasis when the local ablative temperature and thermal energy are not sufficiently high. Additionally, angiogenesis potential induced by RFA-induced hyperthermia also can play a role in the rapid growth of residual tumor cells that have escaped ablation injury (14). This phenomenon is often referred to as a 'malignant transformation', which is associated with RFA therapies used to treat tumors (33). RFA is not only an important therapeutic method, but the microenvironmental conditions present with or induced by RFA can be replicated in *in vitro* cell culture. The cell lines we used were already established and used in previous studies, thus that further spontaneous transformation under normal culture conditions would be unlikely. Therefore, we concluded that the biological microenvironment associated with tumor growth changed due to the exposure to heat stress. Heat-adapted sublines became more proliferative, which became the focus of our subsequent study to identify the molecular biological mechanisms involved in tumor recurrence.

Previous studies indicate that RFA causes profound hypoxia directly adjacent to the ablated area. The presence of hypoxia has been reported in several solid tumors and is related to tumor aggressiveness, proliferation and angiogenesis

potential (34). The increased levels of hypoxia induced by RFA provided an additional growth-stimulating microenvironment for the surviving tumor cells. HIF-1α is a transcriptional factor that is induced by hypoxia and regulates multiple biological processes including angiogenesis, cell proliferation and migration (35). In addition to hypoxia, HSPs are overexpressed at the border of the ablated area. HSP70 is overexpressed under conditions of cellular stress, such as heat activation (36). Kroeze *et al* proposed that despite various conflicting results on the influence of HSP70 on damaged cells there is strong evidence indicating that HSP70 overexpression plays an important role in increased cell survival through the recovery of damaged cells, induction of cell proliferation and inhibition of apoptosis (37). Increased expression of HSP70 in surviving tumor cells at the border of thermally ablated tumors may lead to the development of more aggressive tumor cells (38). Through pull-down assays and peptide arrays, Zhou *et al* confirmed that HSP70 directly binds the oxygen-dependent degradation domain (ODD) of HIF-1α, which initiates PI3K/Akt-mediated degradation of HIF-1α under hypoxic conditions. These data suggest that HSP70 constitutes an integral player in HIF-1α accumulation and that PI3K/Akt contributes to HIF-1α stabilization by provoking the expression of HSP70 (39). This agrees with our results that hyperthermia-induced lung cancer cells exhibited enhanced proliferation and angiogenesis potential through the PI3K/Akt/HSP70/HIF-1α signaling pathway. *In vivo* the peripheral region around the ablation zone highly expressed HSP70/HIF-1α. When a specific inhibitor of PI3K/Akt was applied *in vitro* and *in vivo*, the proliferation activity and angiogenesis potential were both inhibited, regardless of cell type.

RFA has been proposed as an acceptable alternative treatment for lung cancer. Although the technique and condition of ablation have steadily improved, including the application of multipolar ablation and widening of the ablation margin, local recurrence is still common. Multidisciplinary synthetic therapy, which can combine RFA with other treatments, is also recently a subject of increased interest. The present study demonstrated that RFA-induced hyperthermia inherently changes the properties of cells, creating different cancer sublines. These sublines exhibited enhanced viability, proliferation and angiogenesis potential. The PI3K/Akt/HSP70/HIF-1α signaling pathway played a central role during this biological process. Therefore, RFA therapy supplemented by molecular therapy targeting PI3K/Akt/HSP70/HIF-1α signaling may decrease the incidence of local recurrence, improving patient prognosis. The present study supplies additional theoretical basis for the use of multidisciplinary synthetic therapies to treat lung cancer.

Acknowledgements

The present study was funded by the National Nature Science Foundation of China (no. 81302028). We would like to thank the Research Center of the First Affiliated Hospital of Anhui Medical University and the Laboratory Animal Center of Anhui Medical University for providing technical assistance. The authors would like to thank the Duoease Scientific Service Center for excellent language editing service and suggestions for figure revision.

References

1. Ferlay J, Shin HR, Bray F, Forman D, Mathers C and Parkin DM: Estimates of worldwide burden of cancer in 2008: GLOBOCAN 2008. Int J Cancer 127: 2893-2917, 2010.
2. Chen WQ, Zhang SW, Zou XN and Zhao P: An analysis of lung cancer mortality in China, 2004 - 2005. Zhonghua Yu Fang Yi Xue Za Zhi 44: 378-382, 2010 (In Chinese).
3. Chen W, Zhang S and Zou X: Estimation and projection of lung cancer incidence and mortality in China. Zhongguo Fei Ai Za Zhi 13: 488-493, 2010 (In Chinese).
4. Mohammed TL, Chowdhry A, Reddy GP, Amorosa JK, Brown K, Dyer DS, Ginsburg ME, Heitkamp DE, Jeudy J, Kirsch J, *et al*; Expert Panel on Thoracic Imaging: ACR appropriateness criteria® screening for pulmonary metastases. J Thorac Imaging 26: W1-W3, 2011.
5. Varela G and Thomas PA: Surgical management of advanced non-small cell lung cancer. J Thorac Dis 6 (Suppl 2): S217-S223, 2014.
6. Schreiner W, Semrau S, Fietkau R and Sirbu H: Oligometastatic non-small cell lung cancer - surgical options and therapy strategies. Zentralbl Chir 139: 335-341, 2014 (In German).
7. Baisi A, De Simone M, Raveglia F and Cioffi U: Thermal ablation in the treatment of lung cancer: Present and future. Eur J Cardiothorac Surg 43: 683-686, 2013.
8. de Baere T, Farouil G and Deschamps F: Lung cancer ablation: What is the evidence? Semin Intervent Radiol 30: 151-156, 2013.
9. Goldberg SN, Gazelle GS, Compton CC and McLoud TC: Radiofrequency tissue ablation in the rabbit lung: Efficacy and complications. Acad Radiol 2: 776-784, 1995.
10. Ahmad A, Chen SL, Kavanagh MA, Allegra DP and Bilchik AJ: Radiofrequency ablation of hepatic metastases from colorectal cancer: Are newer generation probes better? Am Surg 72: 875-879, 2006.
11. Shah DR, Green S, Elliot A, McGahan JP and Khatri VP: Current oncologic applications of radiofrequency ablation therapies. World J Gastrointest Oncol 5: 71-80, 2013.
12. Lanuti M, Sharma A, Willers H, Digumarthy SR, Mathisen DJ and Shepard JA: Radiofrequency ablation for stage I non-small cell lung cancer: Management of locoregional recurrence. Ann Thorac Surg 93: 921-988, 2012.
13. Zavaglia C, Corso R, Rampoldi A, Vinci M, Belli LS, Vangeli M, Solcia M, Castoldi C, Prisco C, Vanzulli A, *et al*: Is percutaneous radiofrequency thermal ablation of hepatocellular carcinoma a safe procedure? Eur J Gastroenterol Hepatol 20: 196-201, 2008.
14. Ke S, Ding XM, Kong J, Gao J, Wang SH, Cheng Y and Sun WB: Low temperature of radiofrequency ablation at the target sites can facilitate rapid progression of residual hepatic VX2 carcinoma. J Transl Med 8: 73, 2010.
15. Seeber LM, Horrée N, Vooijs MA, Heintz AP, van der Wall E, Verheijen RH and van Diest PJ: The role of hypoxia inducible factor-1alpha in gynecological cancer. Crit Rev Oncol Hematol 78: 173-184, 2011.
16. Wan J, Ma J, Mei J and Shan G: The effects of HIF-1alpha on gene expression profiles of NCI-H446 human small cell lung cancer cells. J Exp Clin Cancer Res 28: 150, 2009.
17. Wan J, Chai H, Yu Z, Ge W, Kang N, Xia W and Che Y: HIF-1α effects on angiogenic potential in human small cell lung carcinoma. J Exp Clin Cancer Res 30: 77, 2011.
18. Son WY, Han CT, Hwang SH, Lee JH, Kim S and Kim YC: Repression of *hspA2* messenger RNA in human testes with abnormal spermatogenesis. Fertil Steril 73: 1138-1144, 2000.
19. Huang WJ, Xia LM, Zhu F, Huang B, Zhou C, Zhu HF, Wang B, Chen B, Lei P, Shen GX, *et al*: Transcriptional upregulation of HSP70-2 by HIF-1 in cancer cells in response to hypoxia. Int J Cancer 124: 298-305, 2009.
20. Tikhonova NS, Moskaleva OS, Margulis BA and Guzhova IV: Molecular chaperone Hsp70 protects neuroblastoma SK-N-SH cells from hypoxic stress. Tsitologiia 50: 467-472, 2008 (In Russian).
21. Yeh CH, Hsu SP, Yang CC, Chien CT and Wang NP: Hypoxic preconditioning reinforces HIF-alpha-dependent HSP70 signaling to reduce ischemic renal failure-induced renal tubular apoptosis and autophagy. Life Sci 86: 115-123, 2010.
22. Li B, Wang Z, Zhong Y, Lan J, Li X and Lin H: CCR9-CCL25 interaction suppresses apoptosis of lung cancer cells by activating the PI3K/Akt pathway. Med Oncol 32: 66, 2015.
23. Wen W, Liu W, Shao Y and Chen L: VER-155008, a small molecule inhibitor of HSP70 with potent anti-cancer activity on lung cancer cell lines. Exp Biol Med 239: 638-645, 2014.

24. Na JI, Na JY, Choi WY, Lee MC, Park MS, Choi KH, Lee JK, Kim KT, Park JT and Kim HS: The HIF-1 inhibitor YC-1 decreases reactive astrocyte formation in a rodent ischemia model. Am J Transl Res 7: 751-760, 2015.
25. Kong J, Kong J, Pan B, Ke S, Dong S, Li X, Zhou A, Zheng L and Sun WB: Insufficient radiofrequency ablation promotes angiogenesis of residual hepatocellular carcinoma via HIF-1α/VEGFA. PLoS One 7: e37266, 2012.
26. Xu M, Xie XH, Xie XY, Xu ZF, Liu GJ, Zheng YL, Huang GL, Wang W, Zheng SG and Lü MD: Sorafenib suppresses the rapid progress of hepatocellular carcinoma after insufficient radiofrequency ablation therapy: An experiment in vivo. Acta Radiol 54: 199-204, 2013.
27. Beland MD, Wasser EJ, Mayo-Smith WW and Dupuy DE: Primary non-small cell lung cancer: Review of frequency, location, and time of recurrence after radiofrequency ablation. Radiology 254: 301-307, 2010.
28. Baisi A, Raveglia F, De Simone M and Cioffi U: Palliative role of percutaneous radiofrequency ablation for severe hemoptysis in an elderly patient with inoperable lung cancer. J Thorac Cardiovasc Surg 140: 1196-1197, 2010.
29. Pennathur A, Luketich JD, Abbas G, Chen M, Fernando HC, Gooding WE, Schuchert MJ, Gilbert S, Christie NA and Landreneau RJ: Radiofrequency ablation for the treatment of stage I non-small cell lung cancer in high-risk patients. J Thorac Cardiovasc Surg 134: 857-864, 2007.
30. Kashima M, Yamakado K, Takaki H, Kodama H, Yamada T, Uraki J and Nakatsuka A: Complications after 1000 lung radiofrequency ablation sessions in 420 patients: A single center's experiences. AJR Am J Roentgenol 197: W576-W580, 2011.
31. Giraud P, Antoine M, Larrouy A, Milleron B, Callard P, De Rycke Y, Carette MF, Rosenwald JC, Cosset JM, Housset M, *et al*: Evaluation of microscopic tumor extension in non-small-cell lung cancer for three-dimensional conformal radiotherapy planning. Int J Radiat Oncol Biol Phys 48: 1015-1024, 2000.
32. Abbas G, Schuchert MJ, Pennathur A, Gilbert S and Luketich JD: Ablative treatments for lung tumors: Radiofrequency ablation, stereotactic radiosurgery, and microwave ablation. Thorac Surg Clin 17: 261-271, 2007.
33. Obara K, Matsumoto N, Okamoto M, Kobayashi M, Ikeda H, Takahashi H, Katakura Y, Matsunaga K, Ishii T, Okuse C, *et al*: Insufficient radiofrequency ablation therapy may induce further malignant transformation of hepatocellular carcinoma. Hepatol Int 2: 116-123, 2008.
34. Seeber LM, Horrée N, van der Groep P, van der Wall E, Verheijen RH and van Diest PJ: Necrosis related HIF-1alpha expression predicts prognosis in patients with endometrioid endometrial carcinoma. BMC Cancer 10: 307, 2010.
35. Zhao X, Gao S, Ren H, Sun W, Zhang H, Sun J, Yang S and Hao J: Hypoxia-inducible factor-1 promotes pancreatic ductal adenocarcinoma invasion and metastasis by activating transcription of the actin-bundling protein fascin. Cancer Res 74: 2455-2464, 2014.
36. Bhardwaj N, Dormer J, Ahmad F, Strickland AD, Gravante G, Beckingham I, West K, Dennison AR and Lloyd DM: Heat shock protein 70 expression following hepatic radiofrequency ablation is affected by adjacent vasculature. J Surg Res 173: 249-257, 2012.
37. Kroeze SG, van Melick HH, Nijkamp MW, Kruse FK, Kruijssen LW, van Diest PJ, Bosch JL and Jans JJ: Incomplete thermal ablation stimulates proliferation of residual renal carcinoma cells in a translational murine model. BJU Int 110: E281-E286, 2012.
38. Kim EK, Park JD, Shim SY, Kim HS, Kim BI, Choi JH and Kim JE: Effect of chronic hypoxia on proliferation, apoptosis, and HSP70 expression in mouse bronchiolar epithelial cells. Physiol Res 55: 405-411, 2006.
39. Zhou J, Schmid T, Frank R and Brüne B: PI3K/Akt is required for heat shock proteins to protect hypoxia-inducible factor 1alpha from pVHL-independent degradation. J Biol Chem 279: 13506-13513, 2004.